First-principles study of electronic structure and optical properties of heterodiamond BC_2N

Jian Sun, Xiang-Feng Zhou, Ya-Xian Fan, Jing Chen, and Hui-Tian Wang*
National Laboratory of Solid State Microstructures and Department of Physics, Nanjing University, Nanjing 210093, China

Xiaoju Guo, Julong He, and Yongjun Tian
Key Laboratory of Metastable Materials Science and Technology, Yanshan University, Qinhuangdao 066004, China
(Received 29 April 2005; revised manuscript received 3 October 2005; published 10 January 2006)

Heterodiamond BC_2N, as a kind of superhard material expectable, is studied using the *ab initio* pseudopotential density functional method. All the calculations are performed after geometric optimization starting from an eight-atom zinc-blende structure unit cell. For all the structures possible, we calculate in detail the structural parameters, charge transfers, bond populations, band structures, density of states, and optical properties (dielectric function, refractive index, absorption coefficient, reflectivity, electron energy loss spectrum, and photoconductivity). In addition, the optical anisotropy of some structures is also discussed. Our calculated results show that all the structures are metastable and some of them tend to form graphitelike structures and exhibit semimetallic behavior leading to interesting optical properties.

DOI: 10.1103/PhysRevB.73.045108 PACS number(s): 78.20.Ci, 71.15.Mb, 71.20.−b, 81.05.Zx

I. INTRODUCTION

The theoretical exploration and synthesis of ternary boron carbon nitrogen (B-C-N) compounds have been both important and interesting subjects in the field of recent materials, since the theoretical prediction of β-C_3N_4 by Liu and Cohen.[1] The motivations originate mainly from some factors as follows: (i) the ternary B-C-N compounds are expected be superhard and superabrasive with extremely high hardness comparable to the diamond and high thermal stability as cubic boron nitride (c-BN),[2] making the high-density phases of these compounds abrasive and coating materials;[3,4] (ii) the band gap of the B-C-N compounds between the metallic graphite and the insulating hexagonal boron nitride (h-BN) is adjustable by changing the compositions and the atomic arrangement, which has various potential applications such as in full-color display;[5] (iii) the negative electron affinity leads to the promising applications as cold cathode materials for vacuum microelectronic devices and field emission flat panel displays;[6] (iv) to the best of our knowledge, the discovery of superconductivity in the boron-doped diamond also attracts much interest in recent work.[7]

Since the attempt by Badzian in 1981,[8] considerable efforts have been devoted to synthesizing various structured B-C-N compounds.[9–13] Using the high-temperature and high-pressure method, successful synthesis of cubic BC_2N(c-BC_2N) from graphitelike BC_2N has been reported under a pressure above 18 GPa and a temperature over 2200 K.[14] The measured bulk modulus of c-BC_2N is 76 ± 4 GPa,[14] which is higher than c-BN and slightly less than diamond, indicating that it may be a promising superhard material. The first-principles method has been extensively used to study the structural, electronic, and mechanical properties of the B-C-N compounds.[15–18] The optical properties have been rarely reported so far,[19] although they are also of great importance in giving a insight into the fundamental physical properties and potential applications.

II. METHOD

We focus on the heterodiamond BC_2N crystal here, using the *ab initio* pseudopotential density functional method with an eight-atom zinc-blende structure unit cell. All the possible structures are optimized by the BFGS algorithm (proposed by Broyden, Fletcher, Goldfarb and Shannon), which provides a fast way of finding the lowest energy structure and supports cell optimization in the CASTEP code.[20] The optimization is performed until the forces on the atoms are less than 0.01 eV/Å and all the stress components are less than 0.02 GPa, the tolerance in the self-consistent field (SCF) calculation is 5.0×10^{-7} eV/atom. Ultrasoft pseudopotentials are expanded within a plane wave basis set with a 310 eV cutoff energy in the process of optimization. Exchange and correlation effects are shown in the scheme of Perdew-Burke-Eruzerhof (PBE) generalized gradient approximation (GGA). The k-points sampling are $7\times7\times7$ according to the Monkhorst-Pack method, which generates 172 k points in the Brillouin zone. For all the optimized structures, the Mulliken charges and bond populations are investigated in detail with a method that projects plane wave states onto a linear combination of atomic orbitals basis set,[24] which is widely used to perform charge transfers and populations analysis. We also calculated the electronic band structures and density of states (DOS) spectra.

The interaction between photons and electrons can be described in terms of time dependent perturbations of the ground states. The transitions between occupied and unoccupied states are caused by the electric field of the photon. The spectra caused by these excitations can be thought of as a joint DOS between the valence and conduction bands. The imaginary part of the dielectric function, $\varepsilon_2(\omega)$, is calculated from the momentum matrix elements between the occupied and unoccupied wave functions within selection rules. The real part of dielectric function, $\varepsilon_1(\omega)$, can be evaluated from $\varepsilon_2(\omega)$ by the Kramer-Kronig relation. All the other optical properties, including refractive indices, absorption coeffi-

TABLE I. Lattice parameters, cell volume, total energy, and formation energy of the seven structures, compared with *c*-BN and graphite.

Structure	1	2	3	4	5	6	7	*c*-BN	Graphite
a (Å)	3.572	3.570	3.589	3.596	3.931	3.690	3.604	3.595	2.460
b (Å)	3.607	3.566	3.589	3.598	3.593	3.690	3.604	3.595	
c (Å)	3.572	3.610	3.635	3.596	3.931	3.691	4.126	3.595	6.800
α (°)	90	90	90	89.77	78.26	85.92	78.40	90	90
β (°)	90.58	90	90	90.47	102.53	94.07	101.60	90	90
γ (°)	90	90	90	90.23	101.74	94.29	90.35	90	120
Symmetry	$Pmm2$	$P222_1$	$P\bar{4}m2$	Cm	Cm	C2	$C2/m$	$F\bar{4}3m$	$P6_3/mmc$
Volume (Å^3)	46.008	45.964	46.829	46.540	49.016	49.875	51.384	46.462	35.638
E_t (eV/atom)	−165.59	−165.58	−165.12	−165.23	−165.30	−165.21	−165.48	−176.20	−155.96
E_f (eV/atom)	0.390	0.395	0.853	0.744	0.679	0.769	0.495		

cients, reflectivities, optical conductivities, and electron energy loss (EEL) spectra, can be derived from $\varepsilon_1(\omega)$ and $\varepsilon_2(\omega)$.[21]

It should be pointed out that here we used two different kinds of pseudopotentials, ultrasoft and norm-conserving pseudopotentials, in the present paper. We have confirmed that the adoptions of these two pseudopotentials give rise to safely ignorable deviations for the optimized lattice constants and so on, excluding the optical properties. The convergence of ultrasoft pseudopotentials is quicker than that of norm-conserving pseudopotentials and the latter is more suitable than the former to study the optical properties. Therefore, norm-conserving pseudopotentials are chosen to study the optical properties, while ultrasoft pseudopotentials are used for the other calculations (such as structure optimizations, band structures, DOS spectra, and population analyses). In addition, inasmuch as the EEL function in the high energy range is greatly affected by the number of empty bands, norm-conserving pseudopotentials with a high cutoff energy up to 770 eV and 32 empty bands are used to produce reasonable optical properties which cover a wide energy range.

III. RESULTS AND DISCUSSIONS

A. Structural properties and population analyses

The heterodiamond BC_2N structures could be constructed from a *c*-BN unit cell by replacing two B atom and two N atoms by C atoms. Because of the high symmetry of the zinc-blende structure lattice, only seven topologically different structures could be found among the 420 configurations.[18] We first optimized all the seven topologically different structures possible under ambient pressure. Obeying the same rule of sequence in structures as in Ref. 18, we queued the seven structures according to the increasing numbers of B-B and N-N bonds. In Struc-1, Struc-2, and Struc-3, both B-B and N-N bonds are free, Struc-4 and Struc-5 have only N-N or B-B bond free, respectively, while Struc-6 and Struc-7 have no bond free.

In Table I we list the lattice parameters together with the volume of the unit cell, the total energy E_t, and the formation energy $E_f = E_{BC_2N} - (E_{diamond} + E_{c-BN})/2$.[18] The symmetry is lowered to $P1$ when the structure relaxes. The positive formation energies for all seven structures indicate that these structures are metastable and have a tendency to separate into diamond and *c*-BN phases. It is clear that Struc-1 is the lowest in total energy, while Struc-3 has the highest total energy despite it having a high symmetry and contains B-C and C-N bonds only. Above results are in agreement with those of the previous *ab initio* calculations based on the local density approximation (LDA).[18,22] In contrast, the tight-binding molecular dynamics method gave a different conclusion that the Struc-3 has a negative formation energy and the lowest total energy, which leads to a high stability.[23] The lattice parameters of Struc-2 and Struc-4 are almost the same as those given by LDA.[18] Struc-5, Struc-6, and Struc-7 in our calculations are more distorted than those in Sun's work[18] and even deviated comparatively far from the "cubic" structure. Because of the large difference between a (or b) and c listed in Table I, we use the "heterodiamond"[15,19] here, which means "two or more different kinds of elements crystalline in a diamondlike structure" and the heterodiamond should be more pertinent than "cubic".

Struc-1 named as β-BC_2N arouses particular interest, since it exhibits a layer-by-layer structure of N/B/C along the [010] direction, Tateyama *et al.* presented two synthesis paths possible for β-BC_2N (Ref. 15) as direct phase transitions from graphitic BC_2N and from superlattice BN/C_2. The first method has been successfully used to synthesize *c*-BC_2N.[14] After the optimization, we get the lattice parameters of Struc-1 to be $a=c=3.572$ Å and $b=3.607$ Å, which are very close to the results predicted in Ref. 22. Struc-2 ~ -7 can be easily obtained by exchanging the positions of B, C, and N atoms.

Since the ionicity of bonds is a great factor affecting the hardness[4] and the other physical properties of materials, we calculated the charge transfer and bond populations of the seven structures of heterodiamond BC_2N. It is well known that the absolute values of the atomic charges yielded by the population analysis have little physical meaning, since they display a high degree of sensibility to the atomic basis set.

TABLE II. Mulliken charges, bond lengths, and bond populations of the seven structures as well as *c*-BN and graphite. L_B, bond length (Å); P_B, bond populations.

Structure		1	2	3	4	5	6	7	*c*-BN	Graphite
Charge (*e*)	*B*1	0.52	0.51	0.30	0.38	0.57	0.60	0.32	0.64	
	*B*2	0.52	0.51	0.30	0.14	0.57	0.60	0.32		
	*C*1	−0.32	−0.33	−0.07	0.06	−0.12	−0.07	0.03		0
	*C*2	−0.32	−0.33	−0.07	−0.17	0.13	−0.07	−0.04		0
	*C*3	0.19	0.20	−0.07	0.06	−0.12	−0.07	0.03		
	*C*4	0.19	0.20	−0.07	0.07	−0.29	−0.07	−0.04		
	*N*1	−0.39	−0.38	−0.16	−0.27	−0.55	−0.46	−0.31	−0.64	
	*N*2	−0.39	−0.38	−0.16	−0.27	−0.18	−0.46	−0.31		
L_B	*B*-*B*				1.598		2.732	1.625		
(P_B)					(0.67)		(−0.44)	(0.81)		
	N-N					2.718	2.807	2.345		
						(−0.13)	(−0.19)	(−0.04)		
	C-C	1.512	1.525		1.522	1.431	1.555	1.550		1.420
		(0.83)	(0.80)		(0.80)	(1.19)	(0.81)	(0.86)		(1.24)
					1.557		1.582	1.731		2.460
					(0.73)		(0.61)	(0.43)		(−0.35)
	B-C	1.573	1.562	1.566	1.547	1.470	1.575	1.824		
		(0.71)	(0.74)	(0.74)	(0.78)	(1.08)	(0.87)	(0.25)		
					1.562	1.515				
					(0.75)	(1.11)				
	C-N	1.561	1.544	1.555	1.538	1.355	1.456	1.414		
		(0.60)	(0.64)	(0.61)	(0.64)	(0.96)	(0.70)	(0.83)		
					1.544	1.369				
					(0.62)	(0.93)				
					1.598	1.400				
					(0.55)	(0.93)				
	B-N	1.561	1.575		1.569	1.413	1.401	1.444	1.557	
		(0.61)	(0.58)		(0.59)	(0.86)	(1.07)	(0.75)	(0.65)	

However, we still can find some useful information by considering the relative values of Mulliken populations. Table II shows the atomic charges, chemical bond lengths, and bond populations calculated by means of the Mulliken analysis for all the seven different structures. The values of *c*-BN and graphite are also listed in Table II for comparison. For Struc-1, the charges transfer from boron atoms to the neighboring nitrogen and carbon atoms, and from carbon atoms to the nitrogen atoms and the carbon atoms. The Mulliken charges are determined to be $0.52e$ for boron atoms, $-0.39e$ for nitrogen atoms, $-0.32e$ for carbon atoms neighboring with the boron atoms, and $0.19e$ for carbon atoms closing with the nitrogen atoms. The charge transfers between the two bonding atoms in Struc-1 are less than those in the polar covalent *c*-BN, while no charge transfer appears in the pure covalent diamond. The charge transfer in Struc-2 has only a little difference of $0.01e$ from Struc-1 due to their structural similarity. It should be noted that the charge transfer in Struc-3 is the least among the seven structures due to its high symmetry, although its total energy is the highest among the seven structures. This also proves the conclusion that "if cubic BCN were an ordered structure with every B and N atom bonded to a carbon, then the structure would be significantly more covalent."[25]

The bond populations indicate the overlap degree of the electron cloud of two bonding atoms and can be used to access covalent or ionic nature of a chemical bond. For the bond populations, the lowest and highest values imply that the chemical bond exhibits strong ionicity and covalency, respectively. The negative values of bond population for B-B and N-N bonds in Struc-5, Struc-6, and Struc-7 imply that these bonds have the tendency to be broken or have Van der Waals interaction only, just like the interlayer interaction of graphite where the bond populations of the long C-C bonds are −0.35. In addition, the bond populations are over unity for the C-C and B-N bonds in Struc-5 and for the B-C bonds in Struc-7, implying that those bonds collapse "too close" or tend to form sp^2 hybridization as graphite does in which the bond populations of the short C-C bonds in layers are also beyond 1.0. We believe that these structures may be unstable, because the atoms are four-coordinated and are not three-coordinated as the atoms in graphite.

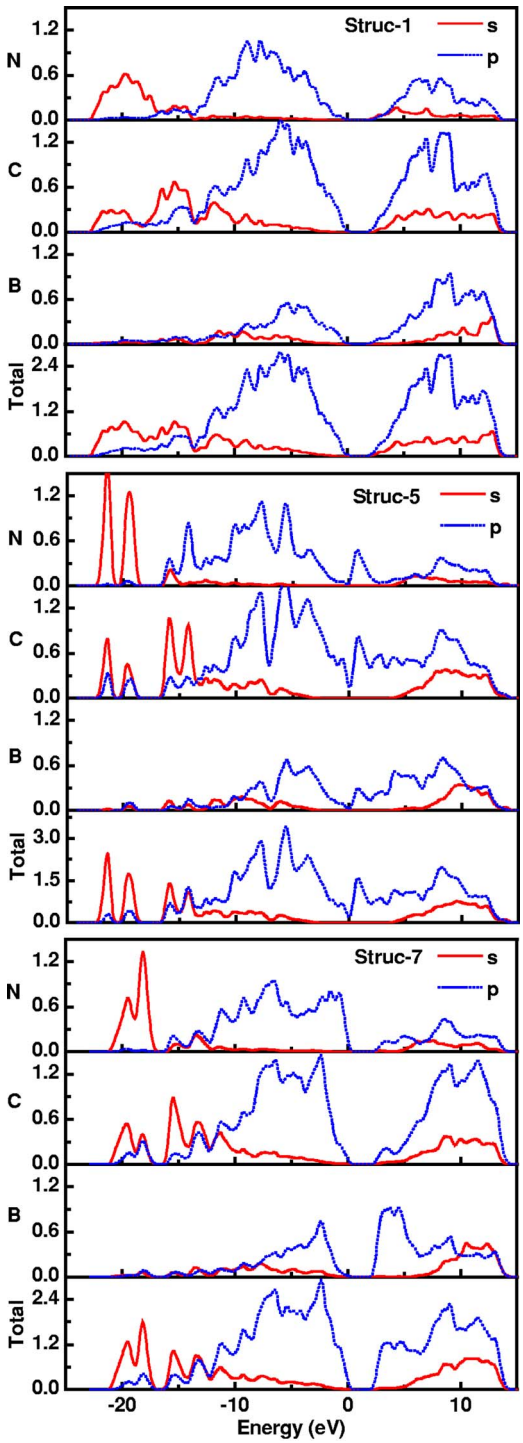

FIG. 1. (Color online) Density of states (DOS) spectra of Struc-1, Struc-5, and Struc-7.

B. Electronic properties

Figure 1 plots the DOS spectra of Struc-1, Struc-5, and Struc-7 only, because Struc-2, -3, and -4 are similar to Struc-1 while Struc-6 is similar to Struc-5 in DOS spectrum. For Struc-1, the conduction bands (CB) originate mainly from the contribution of $2p$ orbitals of B and C atoms, the valence bands (VB) between −23.0 and −13.5 eV are from $2s$ orbitals of C and N atoms. The major contribution to VBs between −13.5 and 0 eV is mainly from N and C $2p$ orbitals. For Struc-5, the VB between −22.5 and −18.5 eV come from $2s$ orbitals of N and C atoms. The VBs between −17 and −13.5 eV belong to the contribution of C $2s$ and N $2p$ orbitals. The electronic density near the Fermi surface and the bottom of CB are mainly from the contributions of C $2p$ and N $2p$ orbitals.

Our GGA results are in agreement with those of the LDA calculations[18] for Struc-1∼-4, which are semiconductors with direct band gaps of 1.9, 2.3, 1.8, and 0.9 eV, respectively. As we know, the computed LDA band gaps of c-BN and diamond are around 4.1 and 4.5 eV, respectively. For the ternary B-C-N compounds produced by mixing the c-BN and diamond, it is thought that, in general, the band gaps should be between 4.1 and 4.5 eV. However, why are the calculated band gaps much lower than the expected values for the BC_2N system? We give some possible explanations here.

(i) The peculiar atom arrangements, especially in Struc-1 and Struc-2, form a layer-by-layer structure that could be considered as a kind of "atom-scale" heterojunction, which might have some band-lineup effects reducing the band gap. The VB top and CB bottom states localized at different species could support this viewpoint.

(ii) The strong B $2p$ and C $2p$ hybridization in the BC_2N system may be the other possible reason. Because of the smaller energy difference between B $2p$ and C $2p$ compared with that for B $2p$ and N $2p$, together with the more extended C $2p$ orbital than that of the N $2p$ orbital, the stronger hybridization will push the B $2p$ level upward. The effect will enhance the VB top to a higher energy.

(iii) N doping in some semiconductors, such as in GaAs,[26] TiO_2,[27] and even in diamond,[28] may heavily narrow the band gap, so the BC_2N system can be regarded as heavily N-doped boron carbides. It can also give us some hints.

After the structural relaxation, the symmetries of Struc-5∼-7 are dramatically changed with respect to the initial zinc-blende structure. In fact, they are closer to the graphite structure rather than cubic. From the band structure and the DOS spectrum, we can find that Struc-5 exhibits semimetal property, as predicted in Ref. 18. As for whether Struc-5 is semiconductor or semimetal, a more accurate method, such as the *GW* approach, is needed to calculate the band gap. Struc-7 has an indirect band gap of about 2.6 eV, which is 0.5 eV larger than the value given by Sun *et al.*[18] It should be noted that the presented results here for graphitelike Struc-5∼-7 might be not very accurate, because the density functional theory (DFT) would encounter some problems when treating the Van der Waals interaction. For all seven structures, the exact band gaps may be larger than the calculated values, as it is well known that the GGA tends to underestimate the band gap.

C. Optical properties

The dielectric function is a very important parameter for a material, because it is the fundamental feature of the linear response to an electromagnetic wave and determines uniquely the propagation behavior of the radiation within.

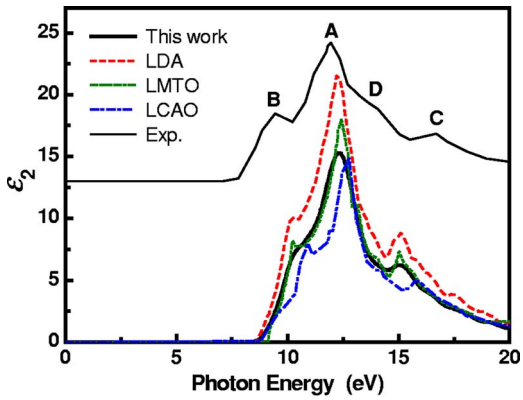

FIG. 2. (Color online) Calculated imaginary part of dielectric functions (thick solid line) of c-BN compared with the LDA result (dash line) in Ref. 29, the LMTO result (dot line) in Ref. 29, and the LCAO result (dash-dot line) in Ref. 30, and the experimental values (thin solid line) in Ref. 31.

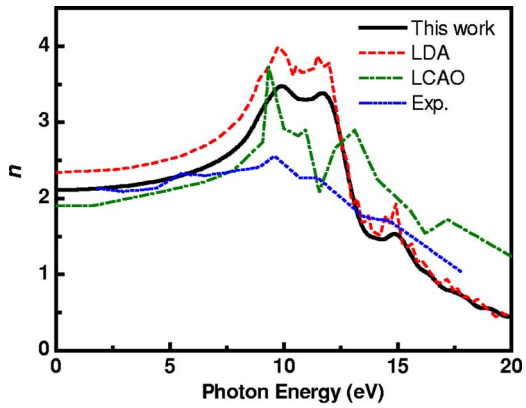

FIG. 3. (Color online) Theoretical refractive index (solid line) of c-BN compared with the LDA result (dash line) in Ref. 29, the LCAO result (dash-dot line) in Ref. 30, and the experimental values (dash-dot-dot line) in Ref. 32.

All the other optical constants could be deduced from the imaginary part $\varepsilon_2(\omega)$ and the real part $\varepsilon_1(\omega)$ of the dielectric function.[19,21] $\varepsilon_2(\omega)$ can be given by calculating the momentum matrix elements between the occupied and unoccupied wave functions with selection rules, and the $\varepsilon_1(\omega)$ can be derived from $\varepsilon_2(\omega)$ by the Kramer-Kronig relationship.

To confirm the reliability of our calculations, we first calculate the imaginary part of the dielectric function of c-BN. As shown in Fig. 2, we compare our result (thick solid line) with the LDA result[29] (dash line), the linear muffin-tin orbital (LMTO) result[29] (dot line), the linear combination of atomic orbitals (LCAO) result[30] (dash-dot line), and the experimental value[31] (thin solid line). The experimental measurement showed two major peaks A and B at 11.8 and 9.1 eV for a crystalline sample. The LCAO result gave the corresponding A and B peaks at 12.6 and 10.7 eV, respectively, having the respective blueshifts of 0.8 and 1.6 eV with respect to the experimental values. The LDA result found the peaks A and B at 12.5 and 9.7 eV, respectively, with the blueshifts of 0.7 and 0.6 eV. The LMTO result showed the peaks A and B at 12.4 and 10.2 eV, respectively, with the blueshifts of 0.6 and 1.1 eV. Our result gives the two peaks at 12.3 and 10.2 eV, respectively, with the blueshifts of 0.5 and 1.1 eV from the experimental values, which is in good agreement with the LMTO result. Figure 3 shows the calculated refractive index of c-BN compared with the experimental measurement[32] and the previous theoretical results.[29,30] Our result agrees with the experiment qualitatively and the LDA result[29] quite well, but we do not find the peak at ~13.0 eV of the LCAO result.[30] We reported the calculated EEL function of c-BN in Fig. 4, together with the experimental measurements[33] and the previous theoretical results.[29,30,34] As we know, the peak in the EEL spectrum originates from a collective oscillation of the valence electrons, classically occurring at a plasmon frequency (determined by $\omega_p^2 = Ne^2/m$, where N is the density of the valence electrons of the sample).[29] Thus, the EEL spectrum can be used to determine c-BN and h-BN phases, because of the different densities between two phases.[33] Our theoretical EEL result for c-BN presents a three-peak structure, which is in good agreement with a recent work[34] discussing the many-body effects in EEL of c-BN by random phase approximation (RPA) including the local field effects (LFE). The first broad peak of our result is located at ~28.7 eV, which is in good agreement with the experimental one (28.5 eV) and the value predicted by Xu and Ching (28 eV). However, the LDA result[29] had a comparatively large value (33.3 eV), which is easily understood that LDA has a tendency to compress the bonds and gives rise to a higher density than experimental value. As a result, the plasmon frequency from LDA is certainly larger than the experimental one and our GGA result. It is well known that in theory the EEL depends mainly on the accuracy of the calculated dielectric functions in the high energy range, as $L(\omega) = \mathrm{Im}[-1/\varepsilon(\omega)] = \varepsilon_2(\omega)/[\varepsilon_1^2(\omega) + \varepsilon_2^2(\omega)]$. Due to the small values of dielectric functions in the high energy range, the inaccuracies (or errors) caused by the different methods lead to the large differences of the calculated EEL functions. Only those calculations having high accuracy for the dielectric function at high frequency can produce reasonable EEL functions and the plasmon frequencies. Our calculated di-

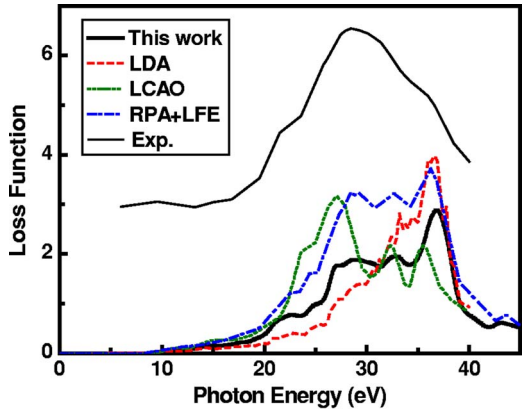

FIG. 4. (Color online) Calculated energy-loss function (thick solid line) of c-BN compared with the LDA result (dashed line) in Ref. 29, the LCAO result (dotted line) in Ref. 30, the RPA plus LFE result (dash-dotted line) in Ref. 34, and the experimental values (thin solid line) in Ref. 33.

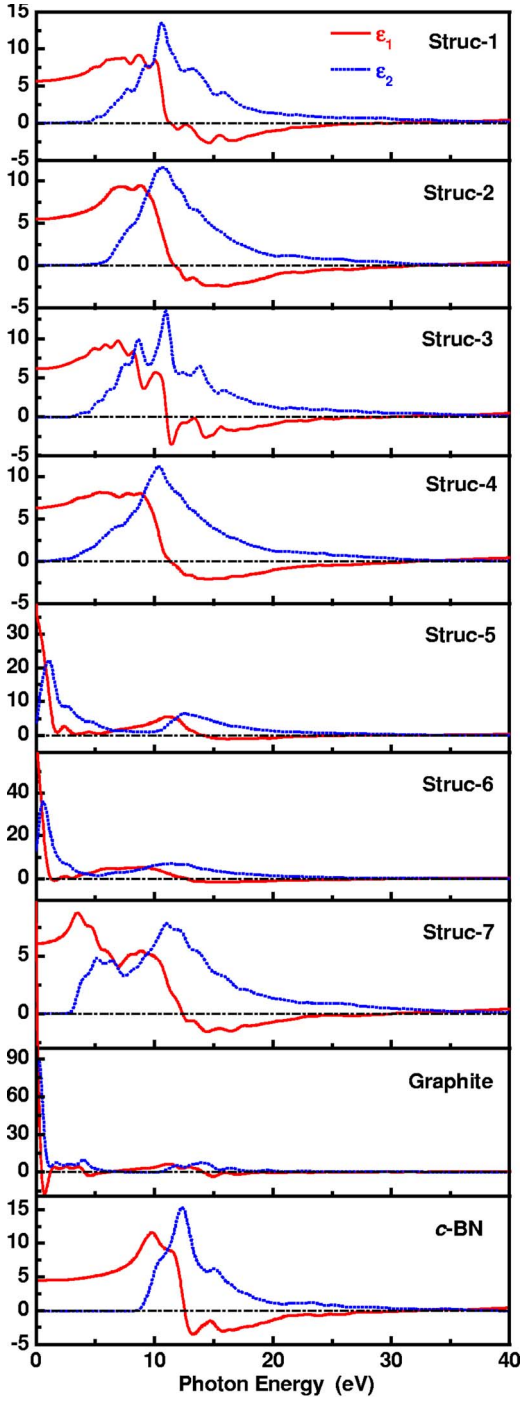

FIG. 5. (Color online) Dielectric functions of polycrystalline heterodiamond BC_2N for the seven structures.

electric function for diamond is also in good agreement with the experimental data (can be found in Ref. 19).

The dielectric functions of polycrystalline phases for all seven structures are plotted in Fig. 5, and the dielectric functions of the *c*-BN and graphite are also given for comparison. The static real parts of the dielectric constants, $\varepsilon_1(0)$, are ~5.3 for Struc-1 and ~5.2 for Struc-2, respectively, which are smaller than 5.5 for the polycrystalline diamond while larger than 4.5 for the polycrystalline *c*-BN. $\varepsilon_1(0)$ of Struc-3, Struc-4, and Struc-6 are ~5.8, ~6.0 and ~5.8, respectively.

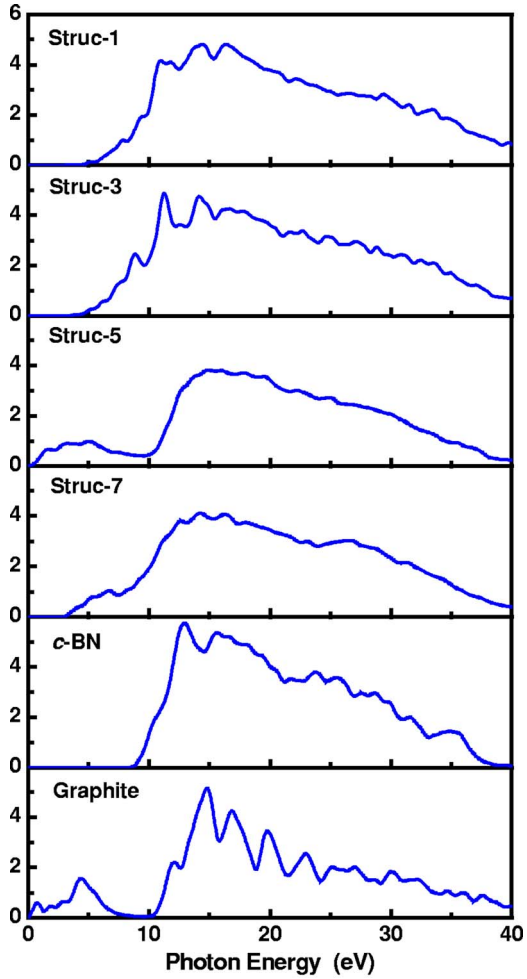

FIG. 6. (Color online) Absorption of polycrystalline Struc-1, Struc-3, Struc-5, and Struc-7, compared with *c*-BN and graphite.

For Struc-5 and Struc-7, $\varepsilon_1(0)$ are very high, as semimetallic materials such as graphite, and decrease rapidly with the increase of the photon energy. We can find from Fig. 5 that, in optical property, three structures (Struc-1, Struc-2, and Struc-4) are similar to *c*-BN; Struc-5 and Struc-6 have similarity to graphite, Struc-3 is slightly different in that there are two prominent peaks in the $\varepsilon_2(\omega)$, and Struc-7 is quite different from all the other six structures. In the following, therefore, we discuss the other optical properties for Struc-1, Struc-3, Struc-5, and Struc-7 only, and make some comparisons with *c*-BN and graphite.

First, we concentrate on the optical properties in polycrystalline structures. Figure 6 shows absorption spectra for the four structures mentioned above, as well as those of the *c*-BN and the graphite. The absorption edges of Struc-1 and Struc-3 are similar to *c*-BN, and have obvious redshifts compared with *c*-BN. Both of them have no absorption in the low energy regime $\hbar\omega < 2.5$ eV, implying that they are always transparent when the wavelength is longer than 170 nm, because such a range of photon energy is just within the forbidden band. In contrast, Struc-5 has an absorption band at a low energy range as graphite, due to their semimetallic

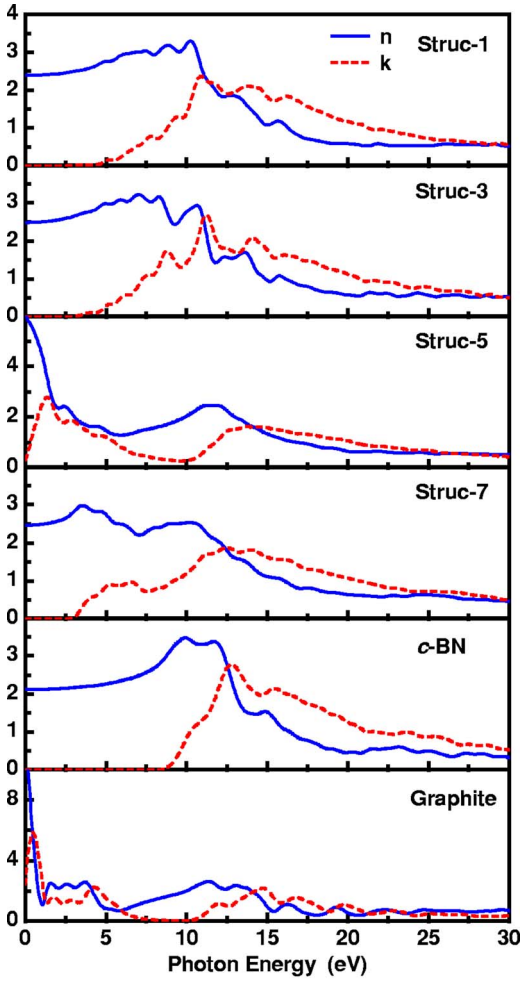

FIG. 7. (Color online) Refractive indices of polycrystalline Struc-1, Struc-3, Struc-5, and Struc-7, compared with c-BN and graphite.

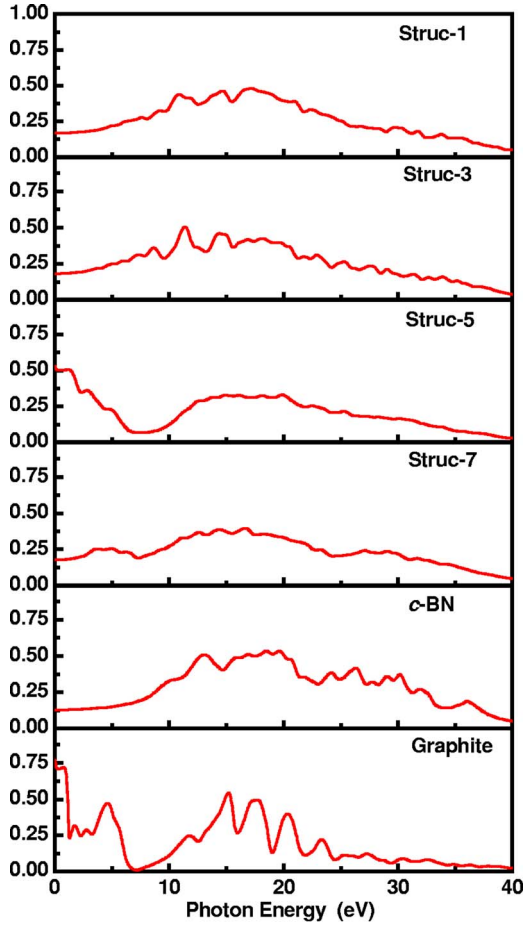

FIG. 8. (Color online) Reflectivity of polycrystalline Struc-1, Struc-3, Struc-5, and Struc-7, compared with c-BN and graphite.

nature. For Struc-7, the absorption edge is redshifted with respect to Struc-1 and c-BN. The absorption of all the seven structures are decreased with the photon energy in the high energy range, where the electron is hard to respond.

From the dispersion curves of refractive indices in Fig. 7, we can find that when the photon energy is zero, among all the seven structures, the refractive index $n(0)$ of Struc-5 has the highest value of $\sim$6.0 that is still lower than that of graphite. For the other structures, the refractive indices $n(0)$ are $\sim$2.3 for Struc-1, $\sim$2.4 for Struc-3, and Struc-7, which are higher than that of c-BN. In the range from 0 to 10 eV, Struc-1 lies in the regime of normal dispersion as c-BN, but Struc-3, Struc-5, and Struc-7 have relatively complicated dispersions. The refractive index of Struc-5 decreases as sharply as graphite, with the increase of photon energy from 0 to 5 eV. Within the range of photon energy from 12.5 to 25 eV, all the seven structures as well as c-BN and graphite belong to the anomalous dispersion in the whole tendency.

The frequency and/or wavelength dependent reflectivities in Fig. 8 indicate that Struc-1 and Struc-3 are very similar to c-BN, while Struc-7 has a weakly broad peak around 5 eV. It seems that Struc-5 has some similarity to graphite in the whole tendency; but the profile of Struc-5 is relatively smooth with respect to graphite, that is to say there are some fine structures in the dispersion curve of reflectivity for graphite. For instance, the reflectivity decreases slowly from 0.5 to 0.1 when the photon energy increases from 0 to 7.5 eV for Struc-5; however, the reflectivity falls off dramatically from 0.9 to 0.1 at $\sim$1.5 eV for graphite, and relatively rapid deductions appear at $\sim$7.2, 16, 19, 22, and 24.5 eV. Therefore, we can assert that for graphite there should be more peaks in the electron loss spectrum.

Figure 9 shows the loss function $L(\omega)$, an important parameter describing the energy loss of a fast electron traversing in the material. The peaks represent the characteristic associated with the plasma resonance and the corresponding frequency is the so-called plasma frequency. The material exhibits dielectric $[\varepsilon_1(\omega)>0]$ and metallic $[\varepsilon_1(\omega)<0]$ behaviors above and below plasma frequency, respectively. There is a broad peak for Struc-1, Struc-3, Struc-7, and c-BN, respectively. Struc-5 has also a relatively small peak at $\sim$6 eV corresponding to the slow descent of reflectivity shown in Fig. 8. For graphite, there are many peaks, which are in agreement with the results predicted from Fig. 8. The plasmon frequencies of Struc-5 and Struc-7 are relatively lower than those of Struc-1 and Struc-3, so EEL may be used to discriminate low- and high-density-phase BC_2N in experiment.

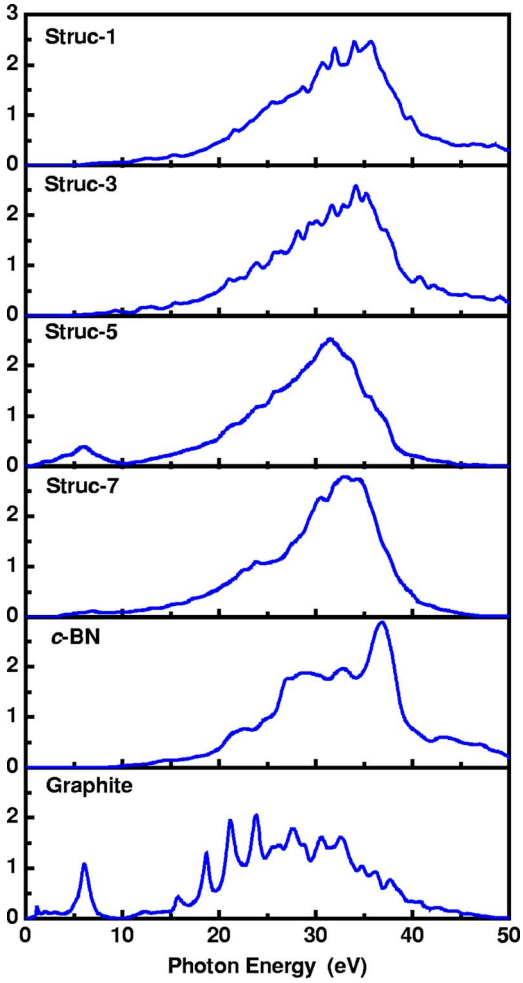

FIG. 9. (Color online) Electron energy-loss functions of polycrystalline Struc-1, Struc-3, Struc-5, and Struc-7, compared with *c*-BN and graphite.

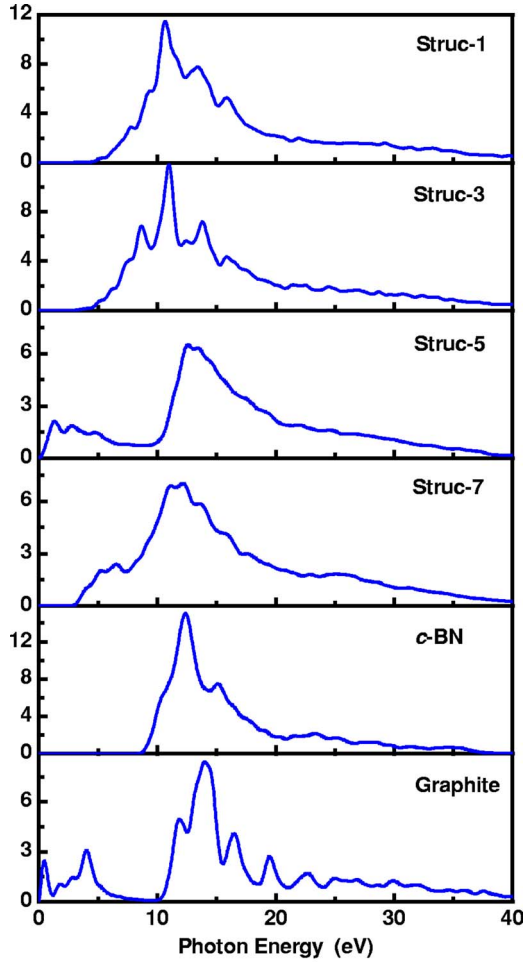

FIG. 10. (Color online) Photoconductivity of polycrystalline Struc-1, Struc-3, Struc-5, and Struc-7, compared with *c*-BN and graphite.

Photoconductivity is the increase in electrical conductivity that results from the increase in the number of free carriers generated when photons are absorbed. The photons must have energy sufficient enough to overcome the band gap in the material. As shown in Fig. 10, there is no photoconductivity when the photon energy is below 2.7 eV for Struc-1, 2.6 eV for Struc-3, and 2.8 eV for Struc-7, because no photon can be absorbed when the photon energy is lower than the band gap. Struc-5 and graphite have almost no band gap, so that the photocurrent can be generated within a wide range of the photon energy.

We now give a brief discussion on the anisotropy of refractive index for Struc-1. The calculated results are plotted in Fig. 11. When the polarization of an electromagnetic wave is perpendicular to the [010] direction, we verify that for all the polarization directions possible (such as along [100] and [001]), the refractive indices are identical and labeled as $n_{[100]}$. If the polarization of an electromagnetic wave is along the [010] direction, the refractive index is different from the above case and named as $n_{[010]}$. It is clear that the refractive index of Struc-1 exhibits anisotropy. Now let us understand such anisotropy from the point view of the crystal optics. Inasmuch as Struc-1 belongs to a tetragonal system, the [010] direction (i.e., *b* axis) is the unique distinguishable (highest symmetric) direction, which is in fact the unique optical axis (i.e., Struc-1 is the uniaxial crystal). In fact, $n_{[100]}$ and $n_{[010]}$ are the ordinary and extraordinary refractive index for Struc-1, n_o and n_e, respectively. In the low energy regime of $\hbar\omega < 5$ and $9\ \text{eV} < \hbar\omega < 13\ \text{eV}$, there exists $n_o < n_e$, meaning that Struc-1 belongs to the positive uniaxial crystal. In the energy regime of $5.5\ \text{eV} < \hbar\omega < 9\ \text{eV}$, Struc-1 should be a negative uniaxial crystal due to $n_o > n_e$. In the two energy regimes stated above, Struc-1 exhibits normal dispersion in the whole tendency, whereas, in the energy regime of $\hbar\omega > 10\ \text{eV}$, Struc-1 exhibits anomalous dispersion in the whole tendency. By the way, the cases of the low symmetric structures such as Struc-5 and Struc-7, as plotted in Fig. 11, are more complicated since they belong to the optically biaxial crystals.

IV. CONCLUSION

Electronic structures and the optical properties of heterodiamond BC_2N were investigated using the *ab initio*

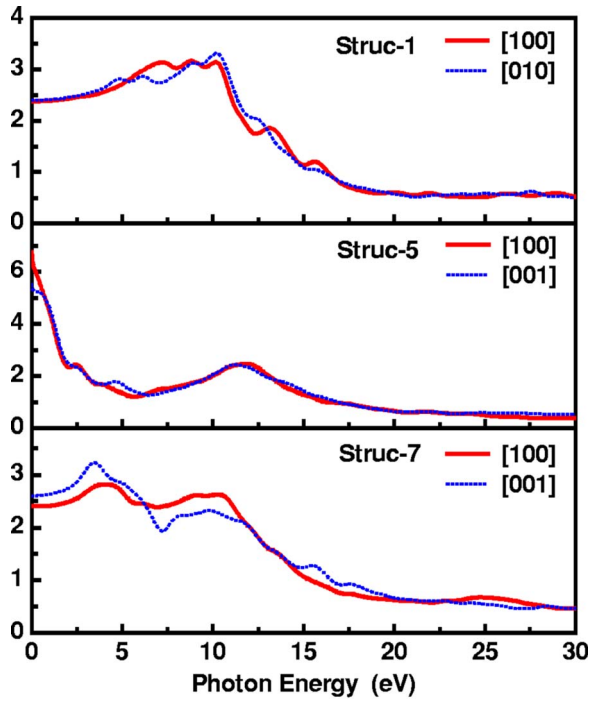

FIG. 11. (Color online) Anisotropic refractive index $n(\omega)$ of Struc-1, Struc-5, and Struc-7.

pseudopotential density functional method. Struc-1, which was named as β-BC_2N in previous papers,[15,22] has the lowest total energy although all the structures seem to be metastable and tend to separate into diamond and c-BN. Struc-5～-7 tend to change into graphitelike structure after geometrical optimization and redefining the lattice. The population analysis indicates that the N-N bonds in Struc-5～-7 and B-B bonds in Struc-6 tend to break, leading to the formations of low-density phase. The studies on the density of electron states, band structures, and the absorption spectrum show that Struc-5 is seemingly semimetal and Struc-5 and Struc-6 are similar to graphite in optical property. The dielectric functions, refractive index, absorption, reflectivity, electron loss function, as well as photoconductivity of Struc-1, Struc-3, Struc-5, and Struc-7 were given in detail. As an example, the anisotropy of refractive index for Struc-1 was also presented. We should note that inasmuch as the present theoretical results are based on the ordered structures of BC_2N and the prepared samples in experiment are mixed by many different phases, so far, the direct comparison between the calculated results and the measured values is difficult. However, our results can still be very useful as references in the future.

ACKNOWLEDGMENTS

The authors gratefully appreciate the helpful discussions from W. Y. Zhang, K. Terakura, W. Y. Ching, G. Cappellini, P. Giannozzi, S. de Gironcoli, and S. Narasimhan. This work was partially supported by National Natural Science Foundation of China (Grant Nos. 10325417, 90101030, 50225207, and 50372055).

*Electronic address: htwang@nju.edu.cn

[1] A. Y. Liu and M. L. Cohen, Science **245**, 841 (1989); A. Y. Liu and M. L. Cohen, Phys. Rev. B **41**, 10727 (1990).
[2] D. M. Teter, MRS Bull. **23**, 22 (1998), and references therein.
[3] E. Byon, J. K. Kim, S. Lee, J. H. Hah, and K. Sugimoto, Surf. Coat. Technol. **169**, 340 (2003).
[4] F. M. Gao, J. L. He, E. R. Wu, S. M. Liu, D. L. Yu, D. C. Li, S. Y. Zhang, and Y. J. Tian, Phys. Rev. Lett. **91**, 015502 (2003).
[5] X. D. Bai, E. G. Wang, J. Yu, and H. Yang, Appl. Phys. Lett. **77**, 67 (2000).
[6] T. Sugino and H. Hieda, Diamond Relat. Mater. **9**, 1233 (2000).
[7] E. A. Ekimov, V. A. Sidorov, E. D. Bauer, N. N. Melnik, N. J. Curro, J. D. Thompson, and S. M. Stishov, Nature (London) **428**, 542 (2004).
[8] A. R. Badzian, MRS Bull. **16**, 1385 (1981).
[9] R. Riedel, J. Bill, and G. Passing, Adv. Mater. (Weinheim, Ger.) **3**, 551 (1991).
[10] S. Itoh, Diamond Relat. Mater. **7**, 195 (1997).
[11] R. Sen, B. C. Satishkumar, A. Govindaraj, K. R. Harikumar, G. Raina, J. P. Zhang, A. K. Cheetham, and C. N. R. Rao, Chem. Phys. Lett. **287**, 671 (1998).
[12] J. Yu, E. G. Wang, J. Ahn, S. F. Yoon, Q. Zhang, J. Cai, and M. B. Yu, J. Appl. Phys. **87**, 4022 (2000).
[13] J. L. He, Y. J. Tian, D. L. Yu, T. S. Wang, S. M. Liu, L. C. Guo, D. C. Li, X. P. Jia, L. X. Chen, G. T. Zou, and O. Yanagisawa, Chem. Phys. Lett. **340**, 431 (2001).
[14] V. L. Solozhenko, D. Andrault, G. Fiquet, M. Mezouar, and D. Rubie, Appl. Phys. Lett. **78**, 1385 (2001).
[15] Y. Tateyama, T. Ogitsu, K. Kusakabe, S. Tsuneyuki, and S. Itoh, Phys. Rev. B **55**, 010161 (1997).
[16] T. Kar, M. Cuma, and S. Scheiner, J. Phys. Chem. A **102**, 10134 (1998).
[17] M. Mattesini and S. F. Matar, Comput. Mater. Sci. **20**, 107 (2001).
[18] H. Sun, S. H. Jhi, D. Roundy, M. L. Cohen, and S. G. Louie, Phys. Rev. B **64**, 094108 (2001), and references therein.
[19] J. Sun, H. T. Wang, N. B. Ming, J. L. He, and Y. J. Tian, Appl. Phys. Lett. **84**, 4544 (2004).
[20] M. Segall, P. Lindan, M. Probert, C. Pickard, P. Hasnip, S. Clark, and M. Payne, J. Phys.: Condens. Matter **14**, 2717 (2002).
[21] S. Saha, T. P. Sinha, and A. Mookerjee, Phys. Rev. B **62**, 8828 (2000); M. Q. Cai, Z. Yin, and M. S. Zhang, Appl. Phys. Lett. **83**, 2805 (2003); J. Sun, H. T. Wang, J. L. He, and Y. J. Tian, Phys. Rev. B **71**, 125132 (2005).
[22] R. Q. Zhang, K. S. Chan, H. F. Cheung, and S. T. Lee, Appl. Phys. Lett. **75**, 2259 (1999).
[23] J. Widany, Diamond Relat. Mater. **7**, 1633 (1998).
[24] D. Sanchez-Portal, E. Artacho, and J. M. Soler, Solid State Commun. **95**, 685 (1995); M. D. Segall, R. Shah, C. J. Pickard, and M. C. Payne, Phys. Rev. B **54**, 16317 (1996).

[25] E. Knittle, R. B. Kaner, R. Jeanloz, and M. L. Cohen, Phys. Rev. B **51**, 12149 (1995).
[26] S. Francoeur, G. Sivaraman, Y. Qiu, S. Nikishin, and H. Temkin, Appl. Phys. Lett. **72**, 1857 (1998); Y. Zhang, A. Mascarenhas, J. F. Geisz, H. P. Xin, and C. W. Tu, Phys. Rev. B **63**, 085205 (2001).
[27] Y. Nakano, T. Morikawa, T. Ohwaki, and Y. Taga, Appl. Phys. Lett. **86**, 132104 (2005).
[28] N. Jiang, A. Hatta, and T. Ito, Jpn. J. Appl. Phys., Part 1 **37**, 1175 (1998).
[29] G. Cappellini, G. Satta, M. Palummo, and G. Onida, Phys. Rev. B **64**, 035104 (2001).
[30] Y. N. Xu and W. Y. Ching, Phys. Rev. B **44**, 7787 (1991).
[31] Y. Osaka, A. Chayahara, H. Yokohama, M. Okamoto, T. Hamada, T. Imura, and M. Fujisawa, in *Synthesis and Properties of Boron Nitride*, edited by J. J. Pouch and S. A. Alteroviz (Trans Tech, Aedermannsdorf, Switzerland, 1990), Vols. 54-55, pp. 277–294.
[32] N. Miyata, K. Moriki, O. Mishima, M. Fujisawa, and T. Hattori, Phys. Rev. B **40**, 12028 (1989).
[33] D. R. McKenzie, W. G. Sainty, and D. Green, Mater. Sci. Forum **54-55**, 193 (1990).
[34] G. Satta, G. Cappellini, V. Olevano, and L. Reining, Phys. Rev. B **70**, 195212 (2004).